Pergamon

0038-1101(94)00123-5

Solid-State Electronics Vol. 38, No. 4, pp. 881–890, 1995
Copyright © 1995 Elsevier Science Ltd
Printed in Great Britain. All rights reserved
0038-1101/95 \$9.50 + 0.00

MONTE CARLO SIMULATION OF HOLE TRANSPORT IN STRAINED $Si_{1-x}Ge_x$

TOSHISHIGE YAMADA and D. K. FERRY

Center for Solid State Electronics Research, Arizona State University, Tempe, AZ 85287-6206, U.S.A.

(Received 4 January 1994; in revised form 27 May 1994)

Abstract—The transport properties of holes in $Si_{1-x}Ge_x$ are studied with a Monte Carlo technique. If the strain is applied to the $Si_{1-x}Ge_x$ channel, it raises the degeneracy of the heavy-hole and light-hole bands: for compressive strain, the heavy-hole band lies at a higher energy than the light-hole band, while for tensile strain, the order reverses, although it is technologically uncertain how to realize the tensile case at this stage. The transport properties are essentially the same for the unstrained and compressive cases, since most holes are in the heavy-hole band over the entire field range of interest. Although the overshot is negligible, the hole velocity is still higher than that of Si, reflecting the excellent hole transport properties in Ge. In the tensile case, we have observed a negative differential resistance region for 5×10^2–5×10^3 V/cm, due to the hole transfer from the light-hole band to the heavy-hole band. The velocity is much larger than that of compressive or unstrained cases, especially at low fields. Because of the small effective mass in the light-hole band, the velocity overshoot is significant in the tensile strain case. These results provide motivation to try to realize the tensile strain case technologically.

1. INTRODUCTION

Recent developments in epitaxial growth techniques of $Si/Si_{1-x}Ge_x$ heterostructures have demonstrated a significant potential of the system for electron device applications[1–3]. In particular, an n-type modulation-doped structure has achieved a mobility of 175,000 cm^2/Vs at 1.5 K[2], and a high-transconductance n-type $Si/Si_{1-x}Ge_x$ modulation doped field-effect transistor has shown 600 mS/mm at 77 K with a gate length of 0.25 μm[3]. This high performance is due to the change of the conduction band structure in a strained Si channel. The strain releases the six-fold degeneracy of the conduction band in Si, and creates two lowered and four raised Δ-valleys[4,5]. Because of this energy split, electrons reside in the lowered Δ-valley preferably, and exhibit a smaller transport mass m_t, which increases the mobility significantly; this split is also responsible for the reduction of the intervalley scattering, resulting in excellent transport properties[6].

In this paper, hole transport in the strain $Si_{1-x}Ge_x$ system is studied by a Monte Carlo technique. This is important especially in engineering applications, such as creation of a complementary circuit with $Si/Si_{1-x}Ge_x$[7]. The Si side is a potential barrier and the $Si_{1-x}Ge_x$ side is a potential well to the holes, regardless of which side is strained and which is relaxed, or if both are strained[4,8]. Thus, channel holes are realized in an inversion layer on the $Si_{1-x}Ge_x$ side. The mobility in Ge is 2000 cm^2/Vs, which is much better than that of Si, 450 cm^2/Vs[9]. The use of a $Si_{1-x}Ge_x$ channel creates a significant advantage over a simple Si channel owing to this excellent hole transport property. The strain has been shown to change the valence-band structure and affects the transport[4,8,10].

The strain at the heterointerface raises the heavy-hole and light-hole band degeneracy. If the strain is compressive, the heavy-hole band is raised and the light-hole band is lowered; if tensile, the light-hole band is raised and the heavy-hole band is lowered[10]. In the latter case, it is expected that the tensile strain will increase the low-field mobility significantly, since most holes reside in the light-hole band and interband scattering is suppressed. This is exactly the mechanism that leads to excellent electron transport in strained Si[6]. Here, the compressive strain will not change the transport properties significantly when compared with the unstrained case, since the light-hole band has a much smaller density of states than the heavy-hole band, and the heavy-hole band primarily determines the transport properties in unstrained Si or Ge[11,12]. This reasoning applies to $Si_{1-x}Ge_x$, too. Therefore, if it is possible to put tensile strain in the $Si_{1-x}Ge_x$ channel, we can make use of high mobility in $Si_{1-x}Ge_x$ and also make the most of the strain effect.

However, the tensile strain cannot be realized by a straightforward gate-metal/doped-Si(barrier)/$Si_{1-x}Ge_x$(channel)/$Si_{1-y}Ge_y$(substrate) structure. The band offset at the heterointerface is such that the Si rich side is a barrier and the Ge rich side is a potential well to the holes[8]. To realize tensile strain in the $Si_{1-x}Ge_x$ channel, we need $x < y$; for compressive stress, we need $x > y$. But for a potential well in the channel, we need $x > y$. Thus, if this conventional structure is used, we can realize only an unstrained

channel or a compressively strained channel where holes are confined, both of which will possess almost the same transport properties for holes, reflecting the heavy-hole band. A new idea has to be introduced to realize the tensile strain case and this is left as an open question for the future.

We study the transport properties of holes in a tensile strained channel, unstrained channel, and a compressive strained channel, and leave the problem as to how they are realized. The study of the tensile case is included since we need to know the maximum performance of this system, and this may provide a motivation to exploit a structure to realize this condition. We concentrate on the study of the strain effect for holes in a $Si_{1-x}Ge_x$ channel, and remove all the unnecessary complications for this purpose. A Monte Carlo technique has been adopted, using a two-band model consisting of heavy-hole and light-hole bands with energy-dependent effective masses[12]. Warping of the valence band, which is important in anisotropic transport at low temperatures[11], is not explicitly included here since we are interested in the average velocity over all directions. Phonon scattering is due to acoustic and optical modes that cause intraband and interband transitions. Alloy scattering is considered based on the model of Ref. [13], and its scattering rate is shown to be orders of magnitude smaller than that of acoustic phonon scattering and not relevant. Acoustic and optical phonons are derived from Si and Ge and are never averaged, but coexist according to the molar fraction of Ge[14]. Acoustic phonon scattering is anisotropic, and angular dependence is different for intraband and interband scattering[15], while optical phonon scattering is known to be isotropic even when the symmetry of the hole wave function is considered[16,17]. Impact ionization is included using Ridley's model for the study of high field transport[18].

Our results show that both the unstrained and compressive case in $Si_{1-x}Ge_x$ exhibit essentially the same velocity-field and energy-field characteristics, which are independent of the strength of the compression and are monotone functions. The velocity and the energy at a given field are between those of Si and Ge, and roughly scale according to the Ge ratio x. This is expected since the light-hole band has much smaller state density and most holes reside in the heavy-hole band as long as the light-hole band is lower in energy than the heavy-hole band. However, in the tensile case where the light-hole band is higher in energy than the heavy-hole band, a drastic change is observed. The velocity-field characteristics show a negative-differential-resistance (NDR), due to the same mechanism as that of NDR in GaAs, which is due to the k-space transfer of holes from the light-hole band to the heavy-hole band at a threshold field[9,19]. The velocity is much larger than that of either compressive or unstrained $Si_{1-x}Ge_x$, reflecting the light effective mass in the light-hole band. These results provide enough motivation to develop a technology to realize tensile strain in the $Si_{1-x}Ge_x$ channel layer and at the same time confine holes there.

In Section 2, the valence band structure is discussed concentrating on the strain effect and the band offset across the heterojunction. In Section 3, the Monte Carlo model with heavy-hole and light-hole bands is explained and in Section 4, the results are presented and discussed. The conclusions are given in Section 5.

2. VALENCE BAND STRUCTURE—STRAIN EFFECT AND BAND LINEUP

In unstrained $Si_{1-x}Ge_x$ with arbitrary x, the valence band is composed of heavy-hole band, light-hole band, and spin-orbit band as shown Fig. 1(a), where the heavy-hole and light-hole bands are degenerate at $\mathbf{k} = 0$. The strain raises the degeneracy of the heavy-hole and light-hole bands at $\mathbf{k} = 0$ and causes a splitting[4,10]. The general valence band structure ($\mathbf{k} \neq 0$) under strain needs numerical evaluation, but the shift of the top of the valence band ΔE_v compared with the unstrained case is calculated analytically by solution of a secular equation of the strain Hamiltonian, for heavy-hole (h.h.), light-hole (l.h.), and spin-orbit (s.o.), respectively, by[4,10]:

$$\Delta E_v(\text{h.h.}) = \varepsilon, \quad (1)$$

$$\Delta E_v(\text{l.h.}) = \tfrac{1}{2}(\varepsilon + \Lambda) + \tfrac{1}{2}\sqrt{9\varepsilon^2 + \Lambda^2 - 2\varepsilon\Lambda}, \quad (2)$$

$$\Delta E_v(\text{s.o.}) = -\tfrac{1}{2}(\varepsilon + \Lambda) - \tfrac{1}{2}\sqrt{9\varepsilon^2 + \Lambda^2 - 2\varepsilon\Lambda}, \quad (3)$$

where ε is the strain energy representing the strength of the strain, with positive values for compressive strain and negative values for tensile strain[10], and Λ is the spin-orbit energy. Figure 1(b) shows this behavior. If compressive, the heavy-hole band is higher, while if tensile, the light-hole band is higher, as schematically shown in the figure. It is reasonable to assume that the effect of strain is to create the energy shifts, and the shape of the valence band structure is the same as that of the unstrained case[20].

It has been reported[4,8] that the band lineup at the heterointerface of $Si/Si_{1-x}Ge_x$ is schematically shown in Fig. 2. Depending on which side is relaxed, we have a type I superlattice for relaxed or strained Si and strained $Si_{1-x}Ge_x$, and a type II superlattice for relaxed $Si_{1-x}Ge_x$ and strained Si. As far as the valence band lineup is concerned, the Si side is *always* a potential barrier and the $Si_{1-x}Ge_x$ side is a potential well to the holes, regardless of which side is relaxed and strained, or if both are strained[4,8]. This is in sharp contrast with that of the conduction band, whose lineup is reversed depending on which side of the heterojunction is relaxed[4,5]. This result can be at least qualitatively generalized to a $Si_{1-x}Ge_x/Si_{1-y}Ge_y$ heterointerface. The valence band lineup is such that the Ge-rich side is a potential well and Si-rich side is a potential barrier to the holes,

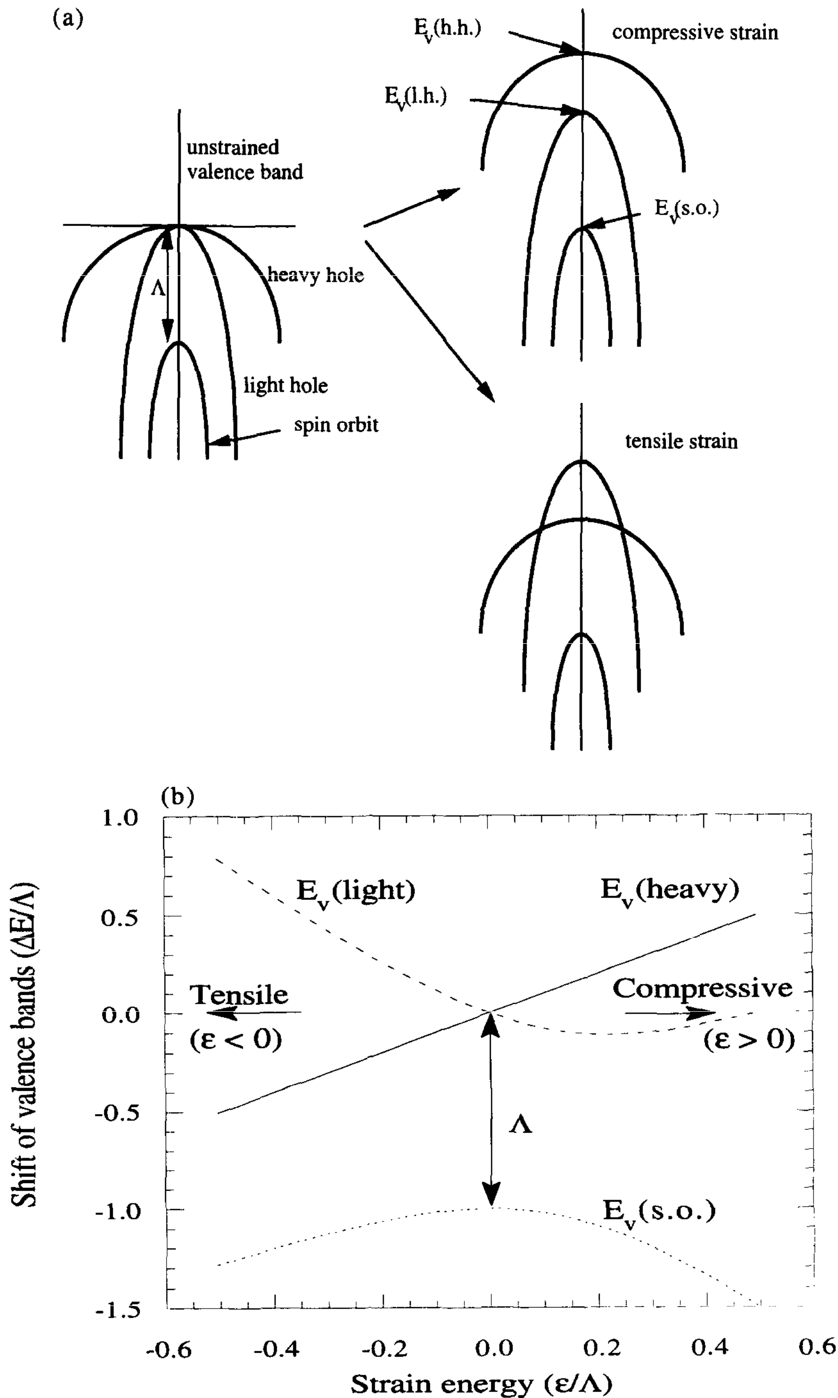

Fig. 1. (a) Valence structure consisting of heavy-hole, light-hole and spin-orbit bands. (b) Shift of the top of each band as a function of strain energy.

regardless of which layer is strained or relaxed, or both are strained.

In a doped-Si/undoped-$Si_{1-x}Ge_x$(channel) $Si_{1-y}Ge_y$(substrate) structure, we can realize compressive strain in the $Si_{1-x}Ge_x$ channel and can keep holes in this channel region for $x > y$, since both Si and $Si_{1-y}Ge_y$ yield a potential barrier and the lattice constant of $Si_{1-x}Ge_x$ adjusts that of $Si_{1-y}Ge_y$. The energy band structure is shown in Fig. 3(a). The unstrained channel of $x = y$ may not be difficult, as shown in Fig. 3(b). The realization of a tensile case with holes in the channel layer is not straightforward. Simple adoption of the above structure will cause the band structure in Fig. 3(c), and holes may not be confined in the planned channel region. Holes reside on the $Si_{1-x}Ge_x$ side of the $Si/Si_{1-x}Ge_x$(channel)

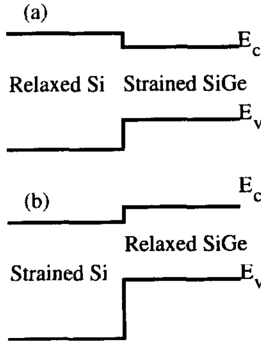

Fig. 2. Band lineup at the $Si/Si_{1-x}Ge_x$ heterojunction.

heterostructure, but some fraction of holes may reside on the $Si_{1-y}Ge_y$ side of heterointerface at $Si_{1-x}Ge_x$(channel)/$Si_{1-y}Ge_y$(substrate).

Nevertheless, the tensile case is of great importance in some applications, due to the higher-lying light-hole band, leading to the enhancement of mobility and NDR. One possibility to create tensile stress and also provide a potential barrier for holes is to search for a substrate material other than $Si_{1-x}Ge_x$ but still compatible with $Si_{1-x}Ge_x$ in the fabrication process. This is left as an open question for future study. In this paper, we study the transport properties of the three cases—tensile, unstrained, and compressive cases assuming that these conditions are successfully realized, and clarify the effect of the strain in the hole transport in $Si_{1-x}Ge_x$. We seek the maximum performance of this system, and may provide a motivation to find a structure to realize this condition. In order to facilitate the following discussion, a quantity ΔE is introduced by:

$$\Delta E = \Delta E_v(\text{l.h.}) - \Delta E_v(\text{h.h.}). \quad (4)$$

As is obvious from the definition, this is the energy splitting between the heavy-hole and light-hole bands and is positive for a compressive case and negative for a tensile case, while $\Delta E = 0$ corresponds to the unstrained case. The strain is characterized by this single parameter, rather than a degree of lattice mismatch, which would require detailed information on how the strain is applied to the channel. If we are interested in a specific structure with a degree of lattice mismatch given, it is possible to convert this to the strain energy ε with the help of the Poisson ratio[10]. Thus, by using (1)–(3), we can convert to the shift of the top of each valence band, and obtain ΔE by (4). As long as a heterojunction $Si_{1-x}Ge_x/Si_{1-y}Ge_y$ or its combination are assumed to create a strain in the channel, there is a technological limit for possible ΔE value, but the following Monte Carlo simulation is confined to $|\Delta E| \leqslant 0.15$ eV, allowing room for future technological progress.

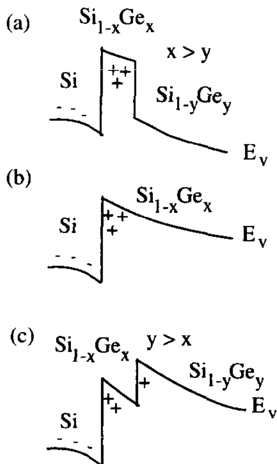

Fig. 3. Energy band of conventional superlattice structure $Si/Si_{1-x}Ge_x/Si_{1-y}Ge_y$.

3. MONTE CARLO MODEL

We use a two-band model for the light-hole and heavy-hole bands. Due to the existence of the spin-orbit band, the parabolic nature of each band is significantly altered to a nonparabolic portion in the energy band around $\Delta/3$[21], while the parabolicity is regained if the absolute value of the hole energy is much larger than this. This effect can be taken into account by assuming a linear dispersion portion in the band structure[12,21]. The effective mass is assumed to be constant below $|E| = 0.1\Delta$, change linearly from 0.1 to 0.3Δ in order to include the effect of spin-orbit band, and again be constant above 0.3Δ in both bands. The effective mass values are taken from Ref. [17], which were averaged over various crystal directions. Our model here may be different from hole Monte Carlo models commonly used[11]. Usually, one warped heavy-hole band model is used to describe the valence band structure and the light-hole band is neglected, due to the large difference between the heavy-hole and light-hole effective mass. In the present case, however, it is essential that heavy-hole and light-hole bands be kept in the model. The warping of the valence band is not considered since we are interested in the strain effects shown in properties averaged over the directions, and are not interested in the anisotropic properties[11]. This encourages us to remove unnecessary complications about warping[22] and allows us to concentrate only on the strain effect.

It has been shown experimentally[14] that in $Si_{1-x}Ge_x$, the original (optical) phonon modes, Si-like modes and Ge-like modes, coexist and are not averaged to bear common phonon modes. The phonon energies in the alloy $Si_{1-x}Ge_x$, are still the same as Si-like phonon mode or Ge-like phonon mode, and their scattering strengths in transport are divided through a linear interpolation of the constituent material values, namely $1-x:x$. Our (optical) phonon model assumes that Si-like modes and Ge-like modes coexist in $Si_{1-x}Ge_x$ and the scattering strengths are given by this constituent ratio $1-x:x$.

The acoustic phonon scattering rate is given by[11,12,17]:

$$1/\tau_{ac} = \frac{k_B T (E_1^0)^2}{2^{1/2}\pi\hbar^4 \rho s^2} m^*(E_k)^{3/2}\sqrt{E_k}, \quad (5)$$

where E_1^0 is an acoustic phonon deformation potential, k_B is the Boltzmann constant, T is the temperature, $\hbar$ is the reduced Planck constant, ρ is the density, s is the sound velocity, E_k is the absolute value of hole kinetic energy, and m^* is the energy dependent effective mass. This $1/\tau_{ac}$ is a factor of two smaller than its counterpart for electrons since the integration of the cell periodic part of the Block function $G(\theta)$ over θ yields 1/2, where θ is an angle between the initial and final momenta of the hole during the scattering event. Acoustic phonon scattering is not isotropic, unlike that of electrons[17]. In fact, the cell-periodic part of the Bloch function is $G(\theta) = 3(\sin^2\theta)/4$ for an interband transition, and $G(\theta) = (1 + 3\cos^2\theta)/4$ for an intraband transition. The final momentum of a hole after the scattering event is determined by using $G(\theta)$ as a probability function in the Monte Carlo process.

Optical phonon scattering is assumed isotropic, following the results of Refs [16] and [17], and $G(\theta) = 1$ is assumed even when the symmetry of the hole wave function is considered. The scattering rate is given by:

$$1/\tau_{op} = \frac{(D_t K)^2}{2^{1/2}\pi\hbar^3 \rho\omega_{op}} [m^*(E_k + \hbar\omega_{op})^{3/2} N_{op} \times \sqrt{E_k + \hbar\omega_{op}} + m^*(E_k - \hbar\omega_{op})^{3/2}(N_{op} + 1) \times \sqrt{E_k - \hbar\omega_{op}}], \quad (6)$$

where $D_t K$ is the optical phonon deformation potential, $\hbar\omega_{op}$ is the optical phonon energy, and N_{op} is the Bose–Einstein function of optical phonons. The second term corresponds to emission and is non-zero only when $E_k > \hbar\omega_{op}$.

Impact ionization is considered using Ridley's model[18]. The scattering rate is given by $1/\tau_{imp} = C(E_k - E_g)^2/E_g^2$, where the numerical constant C is related to the integration of the overlapping integral of the conduction and valence band wave functions, and is determined so that the experimental impact ionization rate is recovered. Holes lose energy equal to the band gap E_g energy after ionization.

Alloy scattering is elastic and can be considered using the model of Ref. [13]; but the estimation shows that the scattering rate ($\sim 10^9$ s^{-1}) is orders of magnitude smaller than that of acoustic phonon scattering ($\sim 10^{13}$ s^{-1}), even for a maximum possible strength of the alloy potential of 1 eV, which is usually on the order of 0.1 eV.

We need to determine deformation potentials and the strength of impact ionization (numerical constant C). The acoustic deformation potential is determined by low field mobility values, 450 cm^2/Vs for Si and 2000 cm^2/Vs for Ge[9]. The optical phonon deformation potential and the numerical factor for impact ionization are determined by the experimental ionization rate reported so far[9,23–25]. The ionization rate at a given field increases with increasing optical phonon deformation potential and the numerical factor of impact ionization. The ratio of both mechanisms is determined by the gradient of the logarithm of the impact ionization rate as a function of the inverse field. The larger the numerical factor is, the smaller the gradient is. Thus, we can determine the strengths of both mechanisms. After choosing deformation potentials and the strength of impact ionization to recover the drift velocity and impact ionization rates for Si hole and Ge hole, we finally obtained the values in Table 1, although we do not exclude another choice of these parameters. Figure 4 shows the velocity-field characteristics of Si hole and Ge hole, with the insertion of mobility lines. Figure 5 illustrates the impact ionization ratio, with some experimental results[9,23–25]. Although our model is simple, the Monte Carlo result is well within the experimental values in both figures. In order to simulate alloys, all the deformation potentials and masses are assumed to be linearly dependent on the Ge fraction x.

4. RESULTS AND DISCUSSION

In Fig. 6, we show the velocity-field characteristics for $Si_{0.5}Ge_{0.5}$ with $\Delta E = 0, \pm 0.1$, and ± 0.15 eV. Figure 7 shows the energy-field characteristics for the condition of Fig. 6, where the absolute value of the total hole energy including ΔE is plotted. The energy is the absolute value of the total energy, where the potential energy is measured from the top of the upper band. Because of the two-band model adopted,

Table 1. Monte Carlo model

	Si	Ref.	Ge	Ref.
$m_h(E/A \ll 1)$	$0.53m_0$	17	$0.346m_0$	17
$m_h(E/A \gg 1)$	$1.26m_0$	17	$0.73m_0$	17
$m_l(E/A \ll 1)$	$0.15\,m_0$	17	$0.042m_0$	17
$m_l(E/A \gg 1)$	$0.36m_0$	17	$0.25m_0$	17
E_1^0	5.0 eV	17	4.6 eV	17
$D_t K$	1.05×10^9 eV	pw[b]	1.6×10^9 eV	pw
Θ_{op}	0.0634 eV	17	0.0371 eV	17
s	6.6×10^3 m/s	17	3.9×10^3 m/s	17
ρ	2.33×10^3 kg/m	17	5.32×10^3 kg/m	17
C	3×10^{12} 1/s	pw	3×10^{12} 1/s	pw

[a]m_0, vacuum electron mass; [b]pw, present work.

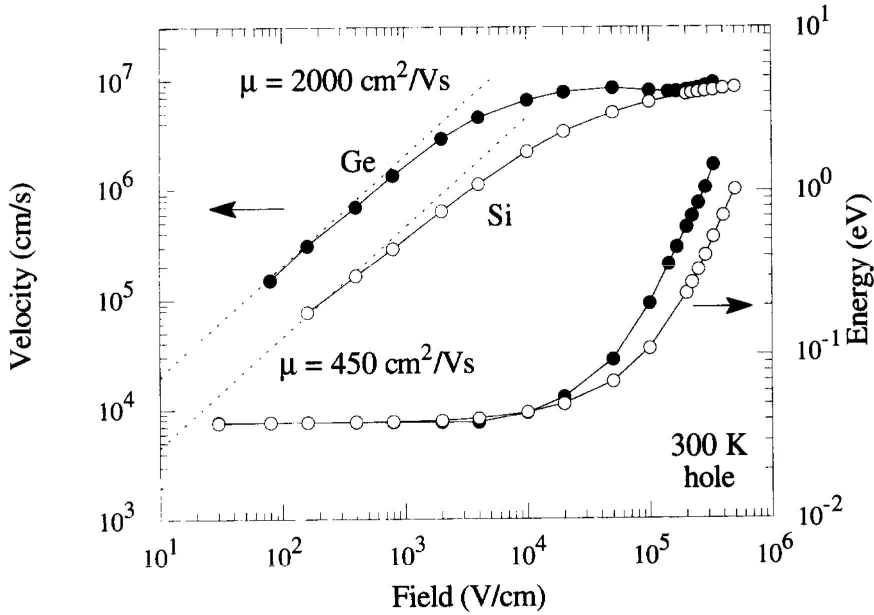

Fig. 4. Velocity-field characteristics of holes in Si and Ge.

the total energy is larger than the thermal energy if substantial number of holes populate the lower band that have potential energy ΔE. This is in fact observed in the figure. For compressive and unstrained cases of $\Delta E > 0$, the energy for $F < \sim 10^3$ V/cm is thermal energy, while it is much larger for tensile cases of $\Delta E < 0$ due to the band split energy. In the unstrained or compressive cases of $\Delta E = 0, 0.1$ and 0.15, the velocity and the energy are a monotone function of the field, with a similar shape to those of Si or Ge in Figs 4 and 5. The functional values at a given field are between those of Si and those of Ge, roughly scale according to the Ge ratio x. This is expected since the light-hole band has a much smaller state density and most holes reside in the heavy-hole band as long as the top of the light-hole band is lower than that of the heavy hole band. However, in the tensile cases of $\Delta E = -0.1$ and -0.15 eV, where the top of the light-hole band is higher that that of the heavy-hole band, a drastic change is observed. The velocity-field characteristics show NDR around 5×10^2–5×10^3 V/cm, due to the same mechanism as that of NDR in GaAs[9,19]. This is the k-space transfer of holes from the light-hole band to the heavy-hole band at a certain threshold field. The total energy measured from the highest point of the va-

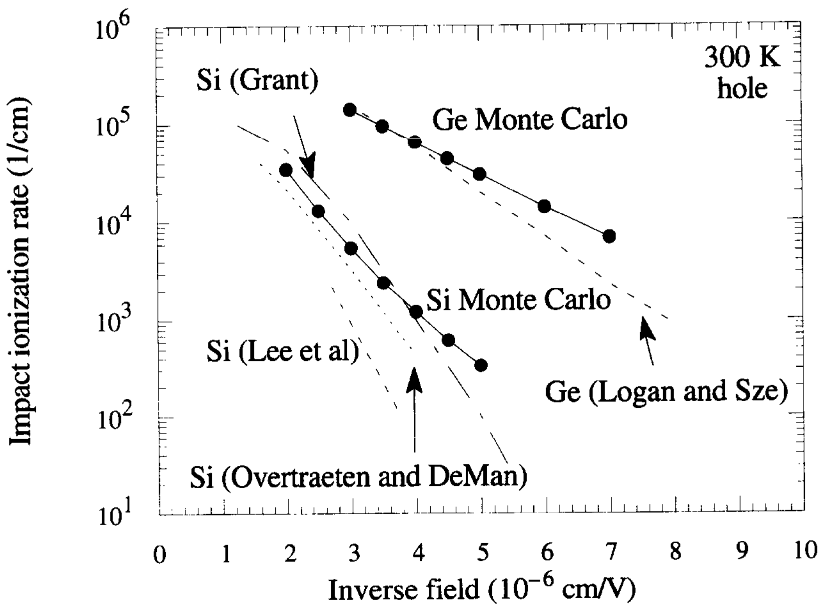

Fig. 5. Impact ionization rate as a function of the field for holes in Si and Ge.

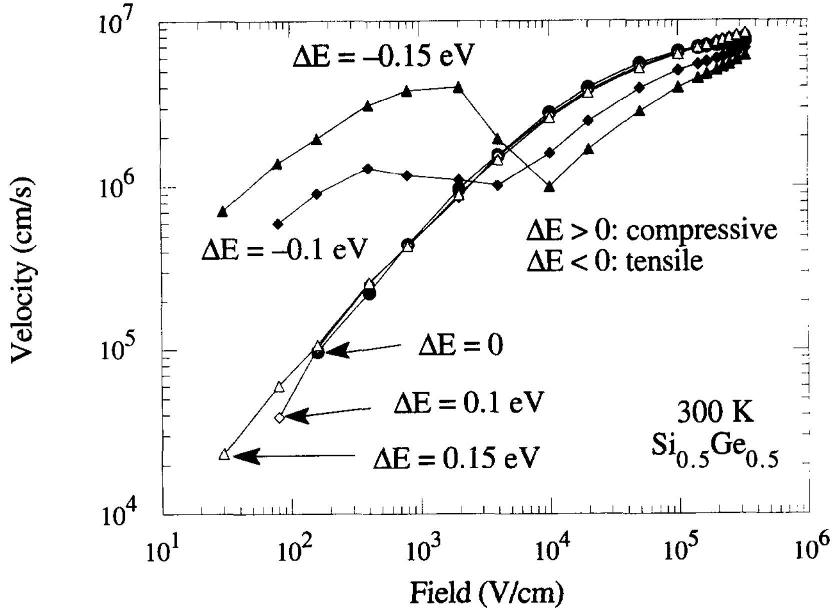

Fig. 6. Velocity-field characteristics of holes in $Si_{0.5}Ge_{0.5}$ with $\Delta E = 0$, ± 0.1 and ± 0.15 eV.

lence band increases significantly. Because of k-space hole transfer, the velocity characteristics for the tensile case is nonlinear down to extremely low fields around $F \sim 10^2$ V/cm. It is linear for lower fields. Low-field mobility for tensile strained case is quite high, on the order of 10^4 cm^2/Vs, and this is due to a much smaller light-hole effective mass compared to the heavy-hole mass.

This k-space transfer is best seen in the population in heavy-hole and light-hole bands as a function of the field shown in Fig. 8. In the tensile cases of $\Delta E < 0$, a crossover of the heavy-hole population and the light-hole population is observed between 5×10^2 and 5×10^3 V/cm. The light-hole band population is not necessarily larger than that of the lower heavy-hole band even in the nearly equilibrium situation, if an appropriately averaged state-density in the heavy-hole bands is of the same order as the Boltzman factor $\exp(-|\Delta E|k_B T)$ multiplied by an appropriately averaged state density of the light-hole bands, such as the case of $\Delta E = -0.1$ eV. For clear NDR behavior in the velocity-field characteristics, it is required that most holes be in the upper light-hole band in thermal equilibrium, which is in our case $\Delta E \leqslant -0.15$ eV. This is in contrast to the unstrained or compressive cases, where the heavy-hole band population is always much larger than the light-hole band population.

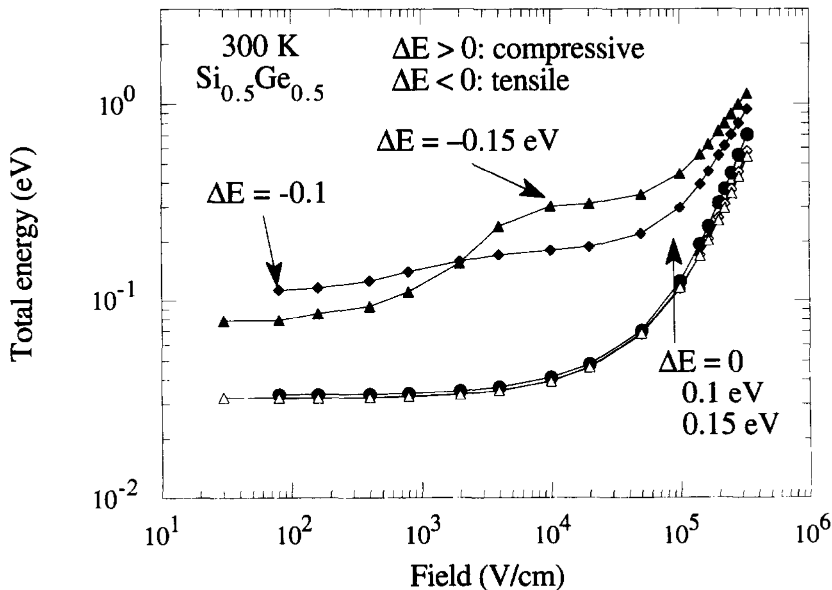

Fig. 7. Energy-field characteristics under the condition of Fig. 6.

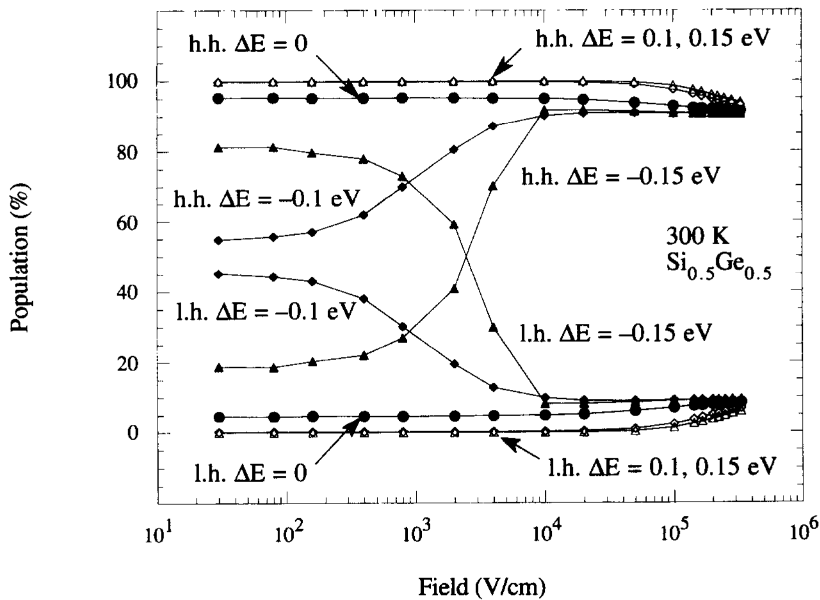

Fig. 8. Band population plot corresponding to Fig. 6.

Figure 9 shows the impact ionization rate. The ionization rate increases for tensile strain, while it decreases for compressive strain, and this tendency is consistent with the result of Fig. 7, where the total average energy is a monotone decreasing function of ΔE for $F > \sim 10^4$ V/cm. We note that this tendency is complementary to the characteristics of ionization rate of electrons in a strained Si layer, which increases with compressive strain[6].

In Fig. 10, we show the velocity-field characteristics for $Si_{1-x}Ge_x$ of various concentrations ($x = 0.25$, 0.5 and 0.75) with $\Delta E = \pm 0.1$ eV. Figure 11 shows the energy-field characteristics corresponding to Fig. 10. The compressive and tensile strain effect is the same for different Ge ratio x. The effect of changing x is to increase the velocity over the entire range of the field, reflecting the superior hole transport properties in Ge to those in Si. The energy for $F > \sim 10^4$ V/cm increases with x, while there is practically no difference in energy for $F < \sim 10^4$ V/cm.

Figure 12 illustrates velocity overshoot in the transient response for $Si_{0.5}Ge_{0.5}$ with $\Delta E = 0.0, \pm 0.1$ and ± 0.15 eV for a sudden application of $F = 5 \times 10^4$ V/cm. There is practically no velocity overshoot for the unstrained case or for the compressive cases of $\Delta E = 0$, 0.1 and 0.15 ev. A significant overshoot is observed in the tensile case, where the peak velocity values are 2.3×10^7 cm/s

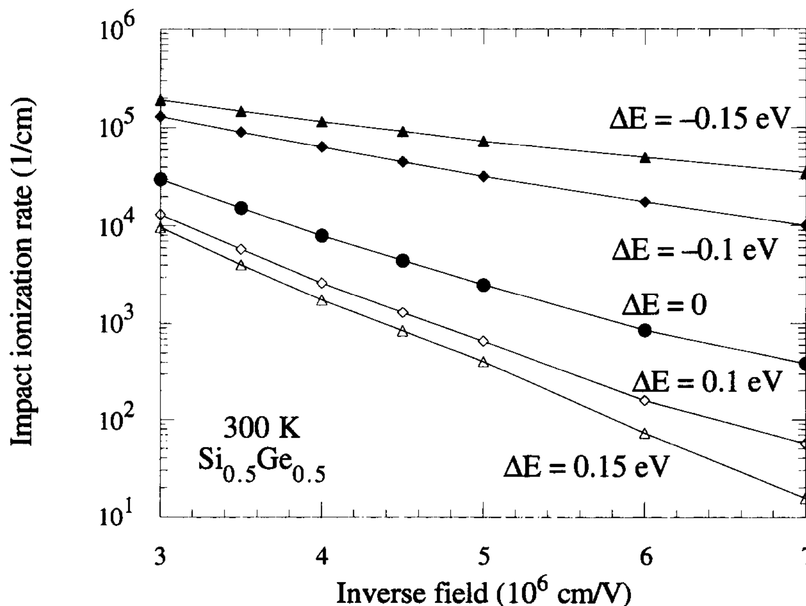

Fig. 9. Impact ionization rate corresponding to Fig. 6.

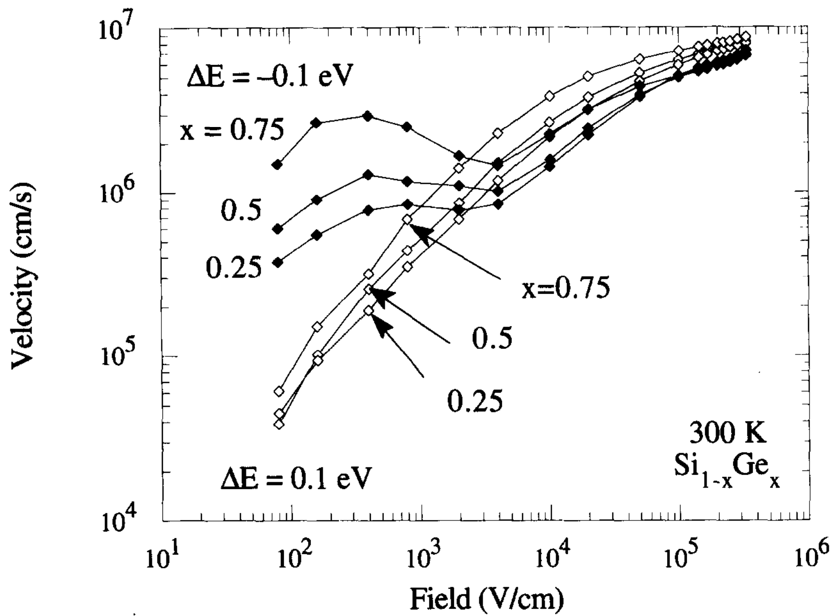

Fig. 10. Velocity-field characteristics for $Si_{1-x}Ge_x$ with $\Delta E = \pm 0.1$ eV.

for $\Delta E = -0.1$ eV and 2.7×10^7 cm/s for $\Delta E = -0.15$ eV. These values are four to five times higher than the steady-state velocity values. The overshoot duration period is about 0.3 ps, which is comparable to that of electrons in a strained Si layer at the same field[6]. In engineering applications, this velocity overshoot is significant and this provides enough motivation to develop a method to realize the tensile strain for confining holes in the channel region, which would lead to a high-performance p-channel field-effect transistor (FET) and enable the creation of complementary circuit based on $Si_{1-x}Ge_x$ technology.

5. CONCLUSIONS

The transport properties of holes in $Si_{1-x}Ge_x$ are studied with a Monte Carlo technique. If the strain is applied to the $Si_{1-x}Ge_x$ channel, it releases the degeneracy of the heavy-hole and light-hole bands: for compressive strain, the heavy-hole band lies higher than that of light-hole band, while for tensile strain, the order is reversed, although technologically it is uncertain how to realize the tensile case at this stage. While no one knows how to realize the tensile strain for SiGe hole channel, it has been shown that the tensile strain is realizable in strained Si hole channel[26]. The transport properties are essentially

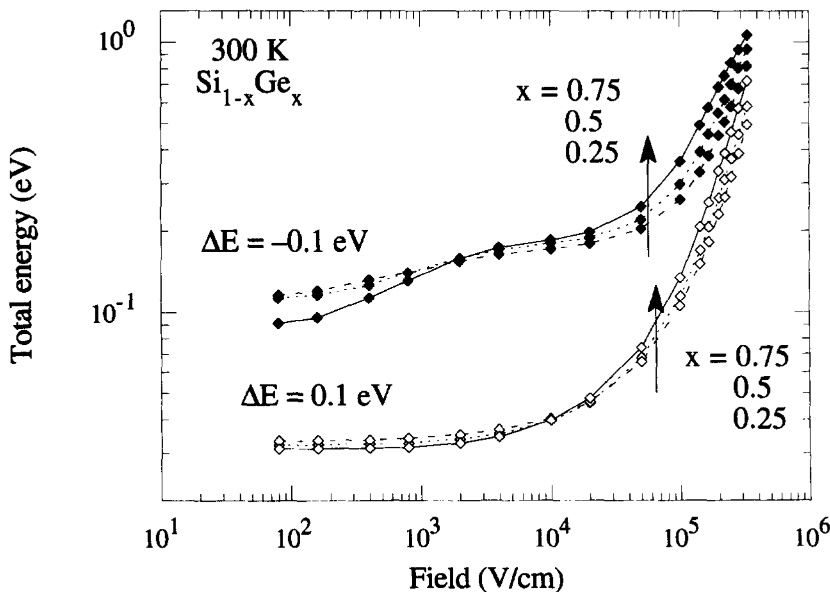

Fig. 11. Energy-field characteristics corresponding to Fig. 10.

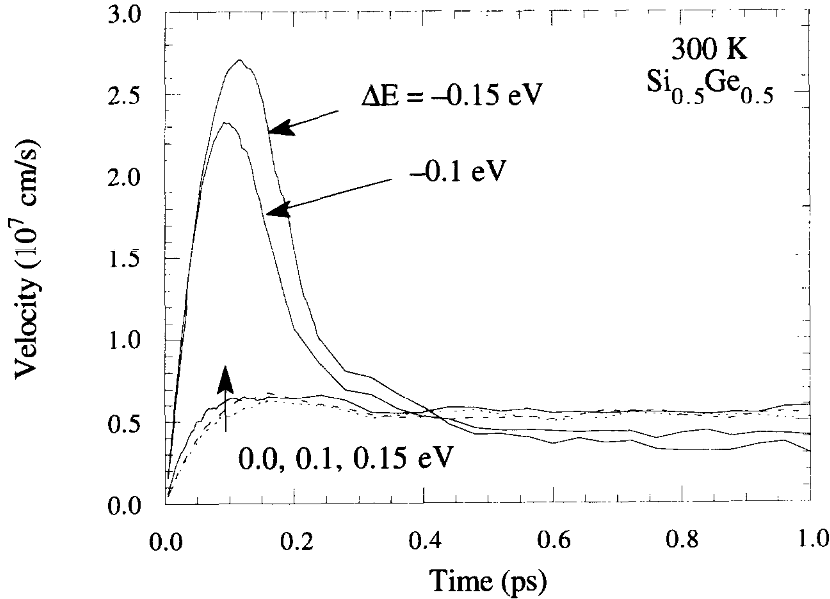

Fig. 12. Velocity overshoot of holes in $Si_{0.5}Ge_{0.5}$ for $F = 5 \times 10^4$ V/cm.

the same for the unstrained and compressive case, since most holes are in the heavy-hole band over the entire field of interest. The velocity is still higher than that of Si, reflecting the excellent hole transport properties in Ge. In the tensile case, we have observed a NDR region for 5×10^2–5×10^3 V/cm, due to the hole transfer from the light-hole band to the heavy-hole band. The velocity is larger than that of unstrained or compressive cases, especially in low fields. Because of the small effective mass in the light-hole band, the velocity overshoot is significant in the tensile strain case. These results provide enough motivation to exploit the idea to realize the tensile strain case technologically, which would lead to a high-performance p-channel FET.

Acknowledgement—This work is supported in part by the Office of Naval Research.

REFERENCES

1. Y. J. Mii, Y. H. Xie, E. A. Fitzgerald, D. Monroe, F. A. Thiel and B. Weir, *Appl. Phys. Lett.* **59,** 1611 (1991).
2. D. Többen, F. Schäffler, A. Zrenner and G. Abstreiter, *Phys. Rev. B* **46,** 4344 (1992).
3. K. Ismail, B. S. Meyerson, S. Rishton, J. Chu, S. Nelson and J. Nocera, *IEEE Trans. Electron Device Lett.* **13,** 229 (1992).
4. R. People, *IEEE J. Quantum Electron.* **22,** 1696 (1985).
5. G. Abstreiter, H. Brugger, T. Wolf, H. Jorke and H. J. Hezog, *Phys. Rev. Lett.* **54,** 2441 (1985).
6. H. Miyata, T. Yamada and D. K. Ferry, *Appl. Phys. Lett.* **62,** 2661 (1993); T. Yamada, H. Miyata, J.-R. Zhou and D. K. Ferry, *Phys. Rev. B* **49,** 1875 (1994).
7. J. M. Hinkley and J. Singh, *Phys. Rev. B* **41,** 2912 (1990); T. Manku, J. M. McGregor, A. Nathan, D. Roulston, J.-P. Noel and D. C. Houghton, *IEEE Trans. Electron Devices* **40,** 1990 (1993).
8. R. People, *Appl. Phys. Lett.* **48,** 538 (1986).
9. S. M. Sze, *Physics of Semiconductor Devices.* Wiley, New York, (1981).
10. H. Hasegawa, *Phys. Rev.* **129,** 1029 (1962); R. People, *Phys. Rev. B* **32,** 1405 (1985).
11. Reggiani, C. Canali, F. Nava and G. Ottaviani, *Phys. Rev. B* **16,** 2781 (1977); L. Reggiani, *J. Phys. Chem. Solids* **37,** 239 (1976).
12. G. Ottaviani, L. Reggiani, C. Canali, F. Nava and A. Alberigi-Quaranta, *Phys. Rev. B* **12,** 3318 (1975).
13. J. W. Harrison and J. R. Hauser, *Phys. Rev. B* **13,** 5347 (1976); D. K. Ferry, *Semiconductors.* Macmillan, New York (1991).
14. J. S. Lannin, *Phys. Rev. B* **16,** 1510 (1977).
15. M. Costato and L. Reggiani, *Physica status solidi* (b) **58,** 471 (1973).
16. G. L. Bir and G. E. Pikus, *Soviet Physics-Solid St.* **2,** 2039 (1961).
17. C. Jacoboni and R. Reggiani, *Rev. Mod. Phys.* **55,** 645 (1983).
18. B. K. Ridley, *Semicond. Sci. Tech.* **2,** 116 (1987).
19. W. Fawcett, A. D. Boardman and S. Swain, *J. Phys. Chem. Sol.* **31,** 1963 (1970).
20. M. M. Rieger, Diplomat thesis (Prof. P. Vogl), Technical University Munich (1991) (unpublished).
21. C. Canali, M. Costato, G. Ottaviani and L. Reggiani, *Phys. Rev. Lett.* **31,** 536 (1973).
22. In a cellular-automation transport model, the velocity direction is quantized in the algorithm, typically eight directions in the plane parallel to the field, so that we can consider effectively that the band is modeled as being artificially extremely warped. If the symmetry is not broken, (the quantized velocities are distributed in various directions without destroying symmetry) then we can recover the Monte Carlo results with continuous velocity direction distributions. This example shows that in the present case where only the average quantities are of interest, we can safely neglect the warping effect. See, e.g. K. Kometer, G. Zandler and P. Vogl, *Phys. Rev. B* **46,** 1382 (1992).
23. R. A. Logan and S. M. Sze, *J. Phys. Soc. Jap. Suppl.* **21,** 434 (1966).
24. W. N. Grant, *Solid-St. Electron.* **16,** 1189 (1973).
25. R. van Overstraeten and DeMan, *Solid-St. Electron.* **13,** 583 (1970).
26. D. K. Nayak and S. K. Chun, *Appl. Phys. Lett.* **64,** 2514 (1994).